# Clinical Implications of AAA Commissioning Errors and Ability of Common Commissioning & Credentialing Procedures to Detect Them

by

Andrew Thinnes McVicker

Graduate Program in Medical Physics
Duke University

Date:_____

Approved:

_____
Justus Adamson, Supervisor

_____
Mark Oldham, Chair

_____
Robert Reiman

Thesis submitted in partial fulfillment of
the requirements for the degree of
Master of Science in the Graduate Program in Medical Physics
in the Graduate School
of Duke University

2014

ABSTRACT

Clinical Implications of AAA Commissioning Errors and Ability of Common

Commissioning & Credentialing Procedures to Detect Them

by

Andrew Thinnes McVicker

Graduate Program in Medical Physics
Duke University

Date:_____
Approved:

_____
Justus Adamson, Supervisor

_____
Mark Oldham, Chair

_____
Robert Reiman

An abstract of a thesis submitted in partial
fulfillment of the requirements for the degree
of Master of Science in the Graduate Program in Medical Physics
in the Graduate School of
Duke University

2014

# Abstract

**Purpose:** To test the ability of the American Association of Physicists in Medicine (AAPM) Task Group 119 (TG-119) commissioning process and the Imaging and Radiation Oncology Core (IROC) credentialing to detect errors in the commissioning process for a commercial treatment planning system.

**Methods:** Commissioning errors were introduced into the commissioning process for the Anisotropic Analytical Algorithm (AAA) within the Eclipse Treatment Planning System (TPS). We included errors in MLC Dosimetric Leaf Gap (DLG), MLC Transmission factor, electron contamination modeling parameters, incorrect flattening filter material, input of Tissue Maximum Ratio (TMR) rather than Percent Depth Dose (PDD) curves, and beam profile measurement with an inappropriately large farmer chamber (simulated using sliding window smoothing of the input dose profiles). We evaluated the clinical impact of these errors for a variety of clinical intensity modulated radiation therapy (IMRT) plans by looking at dose received by 99% of the prescribed treatment volume (PTV D99) and mean and max dose to organs at risk (OARs). The different cases included a head and neck plan, low and intermediate risk prostate plans, a Mesothelioma plan, and a scalp plan. Finally, for the errors with substantial clinical impact, we determined the sensitivity of the commissioning & credentialing processes with the TG119 C-shape and IROC IMRT head and neck phantoms. This was

determined by comparing plans before and after commissioning errors were introduced in the commissioning process using the technique suggested by each respective organization. IROC IMRT credentialing includes film analysis at the midpoint between PTV and OAR using a 4mm distance to agreement metric along with a 7% thermoluminescent detector (TLD) dose comparison. The TG119 C-shape IMRT phantom looks at 3 separate dose planes and using gamma criteria of 3% 3mm.

**Results:** The most clinically severe commissioning errors resulted from the importing TMR rather than PDD curves which had over 10% change in dosimetric indices in clinical plans. Other clinically severe changes came from large changes in the Multileaf Collimator Dosimetric Leaf Gap (MLC DLG) with a change of 1mm resulting in up to a 5% change in the primary PTV D99. This resulted in a discrepancy in the IROC TLDs in the PTVs and OARs of 7.1% and 13.6% respectively, which would have resulted in detection. While use of incorrect flattening filter caused only subtle errors (<1%) in clinical plans, the effect was also most pronounced for the IROC TLDs in the OARs (>6%). MLC Transmission Factor errors were clinically relevant with a change in transmission of 0.9% resulting in changes of over 7% in critical organ dose. This resulted in a discrepancy in the IROC PTV TLDs of 2% and 8% in the IROC OAR TLDs. IROC film analysis was insensitive to the commissioning errors implemented as the only error to fail the distance to agreement criteria for film analysis was the TMR input. TG-119 gamma analysis was done using both relative and absolute criteria and only the absolute

gamma analysis was sensitive to commissioning errors, with relative gamma analysis not detecting even the TMR plan with a 3%, 3mm criteria. 3D dosimetric indices were similar in sensitivity to the IROC TLDs and were more sensitive to commissioning errors than the gamma analysis currently done with TG-119 commissioning.

**Conclusion:** The AAA commissioning process within the Eclipse TPS is surprisingly robust to user error. When errors do occur, the IROC TLD criteria and TG-119 commissioning process are effective at detecting them; however the OAR TLDs are the most sensitive to errors despite the IROC currently excluding them from their analysis.

# Contents

# List of Tables

# List of Figures

# Acknowledgements

Justus Adamson, Ph.D.

Mark Oldham, Ph.D.

# 1. Introduction

External beam radiation therapy (EBRT) is a common therapy used for treatment of cancer and is administered to thousands of patients every day. Advances such as multi-leaf collimators (MLCs), 3D conformal radiation therapy (3DCRT), intensity modulated radiation therapy (IMRT), and volumetric modulated radiation therapy (VMAT) have increased both the effectiveness and complexity of radiation therapy. All of these complexities are first modeled within a computerized treatment planning system. Treatment planning systems are used to perform dose calculations and develop a treatment plan to deliver a prescribed dose to the target volume while sparing normal tissue.

With these advances it is important that proper checks and quality assurance (QA) procedures be in place in order to ensure that treatment is delivered properly. Quality assurance procedures are in place for all aspects of the commissioning and throughout the treatment process. These include commissioning of the TPS, commissioning of the linear accelerator, periodic linear accelerator quality assurance, pretreatment IMRT QA, and credentialing by outside institutions. The commissioning of treatment planning systems and their corresponding dose calculations algorithms is a critical step in the treatment process.

The commissioning process for the treatment planning system is especially important because any errors in this process impact all treatment plans that are created

using the planning system. The AAPM publication by Task Group 53 is a guideline for this commissioning process, and provides the framework to allow physicists to design comprehensive and practical treatment planning QA programs for their clinics without prescribing specific tests[3]. In addition, the report by Task Group 119 furthered this initiative by producing quantitative confidence limits as baseline values for commissioning IMRT planning and delivery systems[4]. TG-119 provides various phantom geometries for which an institution can test IMRT in their treatment planning system by creating treatment plans, optimizing, delivering, and verify using dose measurements. TG-119 also reported agreement between calculated dose and film planes for multiple institutions, which can serve as a reference of achievable agreement.

Another means to verify the TPS and IMRT commissioning process is through credentialing processes offered by outside institutions. The most common inter-institutional credentialing is through the Imaging and Radiation Oncology Core (IROC, formerly the RPC). The Radiation Therapy Oncology Group (RTOG) requires credentialing with the IROC prior to participation in their clinical trials involving IMRT delivery. IROC credentialing process is designed to detect any errors that may have occurred during the commissioning of a treatment planning system. The process consists of the IROC sending a phantom with 8 thermoluminescent detectors (TLDs) and film inserted. The institution then simulates and creates an IMRT plan based on the dose

constraints given by the IROC. The institution irradiates the phantom and returns the phantom with the dose measurements and calculated dose for the TLDs and film planes.

Currently there is little data regarding the sensitivity to commissioning errors of IMRT commissioning using the TG-119 guidelines and credentialing via the IROC. However; a number of studies have been done to evaluate the clinical effect of commissioning errors. Work has been done showing that gamma analysis and planar dose comparisons are insufficient in detecting clinically relevant dose errors[18] and that Dose Volume Histogram based QA metrics are more effective than gamma pass rates in pretreatment dose QA[17]. Tolerances have been determined for beam modeling based on equivalent uniform dose (EUD) in clinical plans using multiple beam models in the Pinnacle TPS[8]. Biological consequences of MLC calibration errors have been evaluated. It has also been found that for low modulation plans there is a better chance to catch MLC calibrations errors with 3D gamma measurements rather than ion chamber measurements, whereas for highly modulated plans there is a better chance of catching MLC calibration errors with ion chamber QA rather than with 3D gamma QA[9].

Further studies evaluated the dosimetric impact of MLC leaf position errors on clinical treatment plans and found that systematic MLC errors had considerable impact[10]. In a separate study they evaluated the feasibility of detecting systematic MLC leaf bank errors using a 2D diode array and an on board EPID and found that an absolute dose comparison using a gamma analysis

(3%, 3mm) could detect a 0.5mm error, while a relative comparison of the planar dose was insensitive to errors[11]. To analyze the effect of MLC commissioning errors on clinical volumetric modulated arc therapy (VMAT) plans, methods have been developed and it was found that the clinical effect was dependent on optimization results from the TPS. A correlation was shown between dose error and average leaf gap width[12]. A number of studies have evaluated the sensitivity of 1D & 2D detectors to commissioning & delivery errors. For example it was found that radiochromic film and a diode matrix could only detect systematic MLC errors on the order of 2 mm or above[13].

Both TG-119 commissioning and IROC credentialing use 2D planar dosimetry measurements to evaluate the accuracy of treatment planning systems. Film has high spatial resolution but only samples select planes of the treatment volume, limiting the capability to detect inaccuracies elsewhere within the treatment volume and organs at risk. 3D dosimetry techniques have been developed that can sample the entire 3D dose distribution. Examples of 3D dosimeters include gel and polymer based dosimeters[14]. 3D dosimetry can achieve high spatial resolution and has been applied to a range of radiotherapy energies, modalities, and applications, including verification of IMRT[14, 15, 16]. After

irradiation, the measured 3D dose matrix can be read out from these 3D dosimeters using MRI (in the case of gel dosimeters) or optical tomography[15].

3D dosimetry is well suited for IMRT commissioning with TG-119 and IROC credentialing for a number of reasons: (1) the additional effort required to perform 3D dosimetry over other less comprehensive measurements may be warranted due to the critical need for correct commissioning of the TPS and the potential severity of errors committed during this process. (2) Both the TPS commissioning and credentialing processes are carried out on an infrequent rather than on a recurring basis; hence the additional effort for 3D dosimetry would not affect the clinic workload of recurring quality assurance. (3) In the case of IROC credentialing, the phantom, film planes, and TLDs are already transferred to a central location; hence the 3D dosimetry technology would not need to be disseminated on a widespread scale. However the question remains as to how much benefit 3D dosimetry techniques would provide over current 1D & 2D measurements.

The purpose of this project was to test the ability of the TG-119 guidelines for IMRT commissioning and IROC credentialing to detect errors in the commissioning process of IMRT within a commercial Treatment Planning System (TPS). We also evaluated if using 3D dosimetric indices would increase the sensitivity of IROC credentialing and TG-119 commissioning procedures in detecting commissioning errors.

# 2. Materials and Methods

## *2.1. Overview*

Figure 1 is an overview of the methods used for this study. To measure each QA technique's sensitivity and ability to detect errors, first the errors were implemented in the Eclipse Analytic Anisotropic Algorithm during the commissioning process. One error was implemented at a time to isolate the effect of each individual mistake made during the commissioning process. Once the algorithm was commissioned with an intentional error, the dose for clinical plans was recalculated using the altered algorithm and compared to the original plan to measure the impact that the commissioning error would have clinically. To measure the sensitivity of the IMRT commissioning process and IROC credentialing, the same was done with plans designed on the TG 119 C-Shape and IROC Head and Neck IMRT phantoms. The newly calculated plans were then compared to the original plans and evaluated using their respective criteria to determine the dosimetric effect of each error.

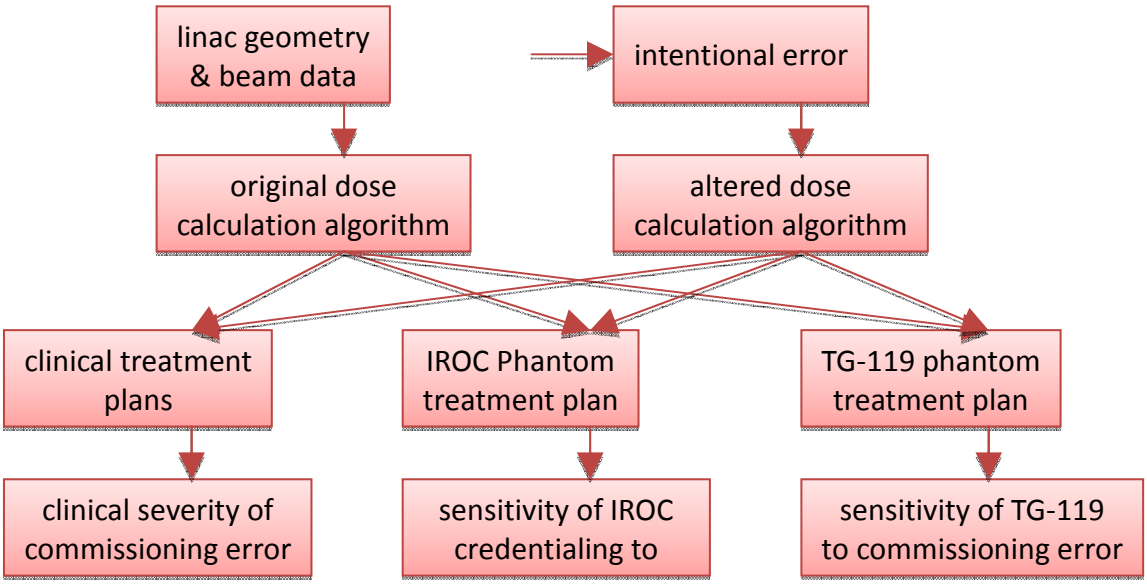


**Figure 1: A schematic of the general procedure.**

## *2.2. Treatment Planning System*

### 2.2.1 Beam Data Input

The beam data requirements include collections of machine specific and geometry specific parameters along with measured beam data. This measured data must all be taken at the same beam geometry and under the same setup conditions for the algorithm to be able to apply it. The measured beam data consists of depth dose curves and profiles using the same field sizes performed on the same axis and with a consistent source-surface distance of between 70 and 140 cm[1]. The beam data used in our configuration was taken at a source-surface distance of 100 cm.

**Table 1: Breakdown of Treatment Planning System commissioning parameters.**

| | |
|---|---|
| Primary | Output Factors<br>Depth Dose Curves<br>Beam Profiles<br>Spectrum Parameters |
| Secondary | Mean Radial Energy<br>Size of Second Source<br>Relative Intensity<br>Mean Energy of Second Source |
| Electron Contamination | Electron Contamination $\sigma 0$<br>Electron Contamination $\sigma 1$<br>Relative Fraction |
| MLC Parameters | Dosimetric Leaf Gap<br>Transmission Factor |

Table 1 shows each of the elements that go into the commission procedure and where they fall in terms of dose contribution. Primary parameters are those used to model the primary source of photons, which consists of bremstrahlung X-rays produced in the target that do not interact in the head of the treatment unit. Secondary parameters are those used in modeling the dose from photons scattered from the flattening filter and collimators, and is modeled as a virtual plane source located at the bottom of the flattening filter. Electron contamination parameters model the dose contribution from electrons generated in the treatment unit head and in air (mainly through Compton scattering). The electron contamination is modeled at the target plane using two Gaussian curves (which determine lateral spread of electrons & field size dependance) and one dose deposition curve which is derived empirically by the beam modeling algorithm as the difference between the largest field size depth dose curves measured

with and calculated without the electron contamination. Finally, the MLC parameters model the complex interactions with the field incident upon the collimator leaves. Electron contamination and MLC parameters are described in more detail in the following sections.

The required measured beam data also includes depth dose curves along the central axis in water taken for field sizes of 4x4 $cm^2$, 6x6 $cm^2$, 10x10 $cm^2$, 20x20 $cm^2$, and for the largest possible field size which for this machine was 40x40 $cm^2$. Additionally recommended and used in our configuration were depth dose curves for the smallest possible field size which was 2x2 $cm^2$, along with curves for 8x8 $cm^2$ and 30x30 $cm^2$. Dose profiles are required from all field sizes at depths of $d_{max}$ (1.5 cm for 6 MV photons), 5 cm, 10 cm, 20 cm, and 30 cm depths. Dose profiles are taken using both inline and crossline scans and for large field sizes diagonal scans are used. For the diagonal scans the tank is offset and only half of the profile is measured. The diagonal scans are then mirrored to create a full dose profile.

The final piece of measured beam data is the output factors. Output factors are typically measured at a depth of 5 cm and are displayed as a ratio of measured dose at depth for each measured field size with respect to the dose at the reference field size of 10x10 $cm^2$. Output factors are required for each of the rectangular field sizes displayed in Table 1. A new table of output factors is then interpolated by the TPS at 1 cm resolution.

**Table 2: Field sizes required for Open Field Output factors[1].**

| Height (FY) \ Width (FX) | S[a] | 3 | 5 | 7 | 10 | 15 | 20 | 30 | 40 | L[b] |
|---|---|---|---|---|---|---|---|---|---|---|
| S | S × S | S × 3 | S × 5 | S × 7 | S × 10 | S × 15 | S × 20 | S × 30 | S × 40 | S × L |
| 3 | 3 × S | 3 × 3 | 3 × 5 | 3 × 7 | 3 × 10 | 3 × 15 | 3 × 20 | 3 × 30 | 3 × 40 | 3 × L |
| 5 | 5 × S | 5 × 3 | 5 × 5 | 5 × 7 | 5 × 10 | 5 × 15 | 5 × 20 | 5 × 30 | 5 × 40 | 5 × L |
| 7 | 7 × S | 7 × 3 | 7 × 5 | 7 × 7 | 7 × 10 | 7 × 15 | 7 × 20 | 7 × 30 | 7 × 40 | 7 × L |
| 10 | 10 × S | 10 × 3 | 10 × 5 | 10 × 7 | 10 × 10 | 10 × 15 | 10 × 20 | 10 × 30 | 10 × 40 | 10 × L |
| 15 | 15 × S | 15 × 3 | 15 × 5 | 15 × 7 | 15 × 10 | 15 × 15 | 15 × 20 | 15 × 30 | 15 × 40 | 15 × L |
| 20 | 20 × S | 20 × 3 | 20 × 5 | 20 × 7 | 20 × 10 | 20 × 15 | 20 × 20 | 20 × 30 | 20 × 40 | 20 × L |
| 30 | 30 × S | 30 × 3 | 30 × 5 | 30 × 7 | 30 × 10 | 30 × 15 | 30 × 20 | 30 × 30 | 30 × 40 | 30 × L |
| 40 | 40 × S | 40 × 3 | 40 × 5 | 40 × 7 | 40 × 10 | 40 × 15 | 40 × 20 | 40 × 30 | 40 × 40 | 40 × L |
| L | L × S | L × 3 | L × 5 | L × 7 | L × 10 | L × 15 | L × 20 | L × 30 | L × 40 | L × L |

a. S = smallest field size
b. L = largest field size

The required general machine parameters include source-axis distance (SAD) as well as the smallest and largest allowable open beam field size in each direction. This is also where information about the profiles is input so that the TPS knows information about the depth at which the profile is taken. The general parameters table is shown in Figure 2. Beyond the general parameters is a second set of parameters that define the absolute dose calibration of the machine. These parameters include machine type, calibration depth and absolute dose at calibration depth.

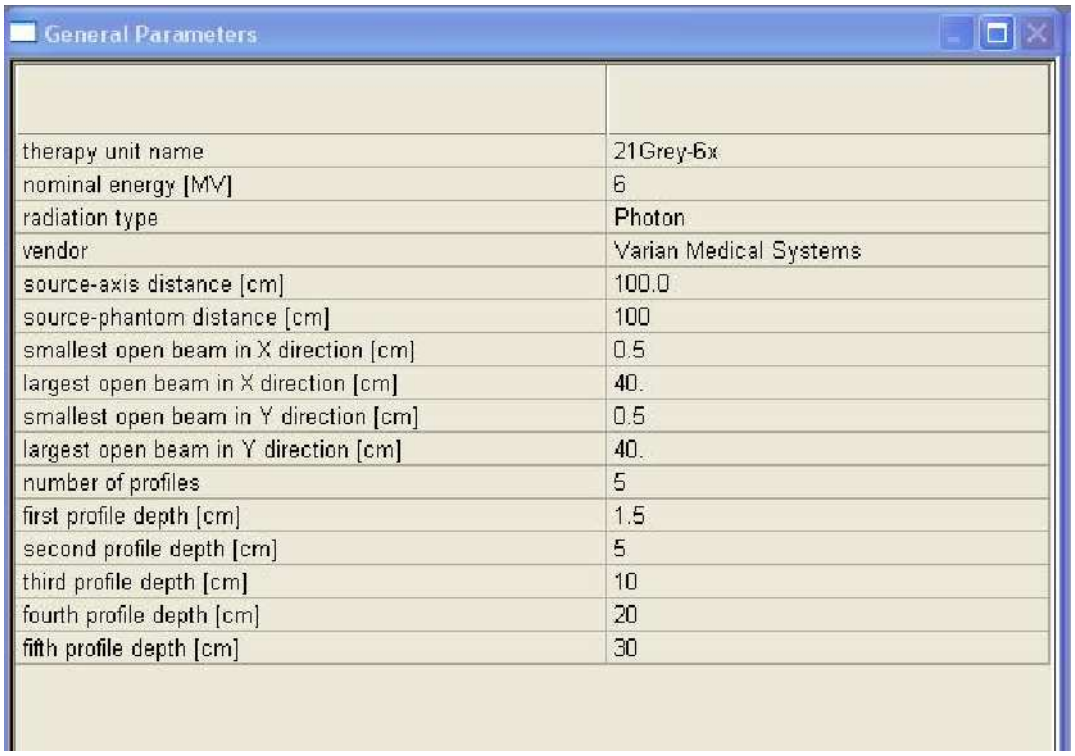


| | |
|---|---|
| therapy unit name | 21Grey-6x |
| nominal energy [MV] | 6 |
| radiation type | Photon |
| vendor | Varian Medical Systems |
| source-axis distance [cm] | 100.0 |
| source-phantom distance [cm] | 100 |
| smallest open beam in X direction [cm] | 0.5 |
| largest open beam in X direction [cm] | 40. |
| smallest open beam in Y direction [cm] | 0.5 |
| largest open beam in Y direction [cm] | 40. |
| number of profiles | 5 |
| first profile depth [cm] | 1.5 |
| second profile depth [cm] | 5 |
| third profile depth [cm] | 10 |
| fourth profile depth [cm] | 20 |
| fifth profile depth [cm] | 30 |

**Figure 2: General Beam Parameters as input into Eclipse.**

### 2.2.2 Calculation of Beam Model

Using this input information and an existing library of machine data, further information is extracted from the machine library and calculated within the AAA beam modeling algorithm such as Mean Radial Energy, Intensity Profiles, Electron Contamination parameters, and spectrum parameters. The mean radial energy and initial photon energy spectrum in the machine parameter library is pre-determined from Monte Carlo simulations of the bremsstrahlung spectrum of electrons incident on the target. Electron contamination is modeled using a 2D Gaussian second source[1]. From

this second source modeling the electron contamination curve is calculated and convolved into dose distribution. Other parameters calculated by the treatment planning algorithm are the Mean Radial Energy Curve, Intensity Profile Curve, and Energy Spectrum. Mean Radial Energy and Intensity Profile are functions of distance off axis, and the Energy Spectrum shows the fluence per energy.

### 2.2.3 Verification

After the AAA beam modeling algorithm is prepared, the TPS allows the user to evaluate the agreement between the calculated and the measured curves. This comparison is done for all input beam profiles, diagonal profiles, and depth dose curves.

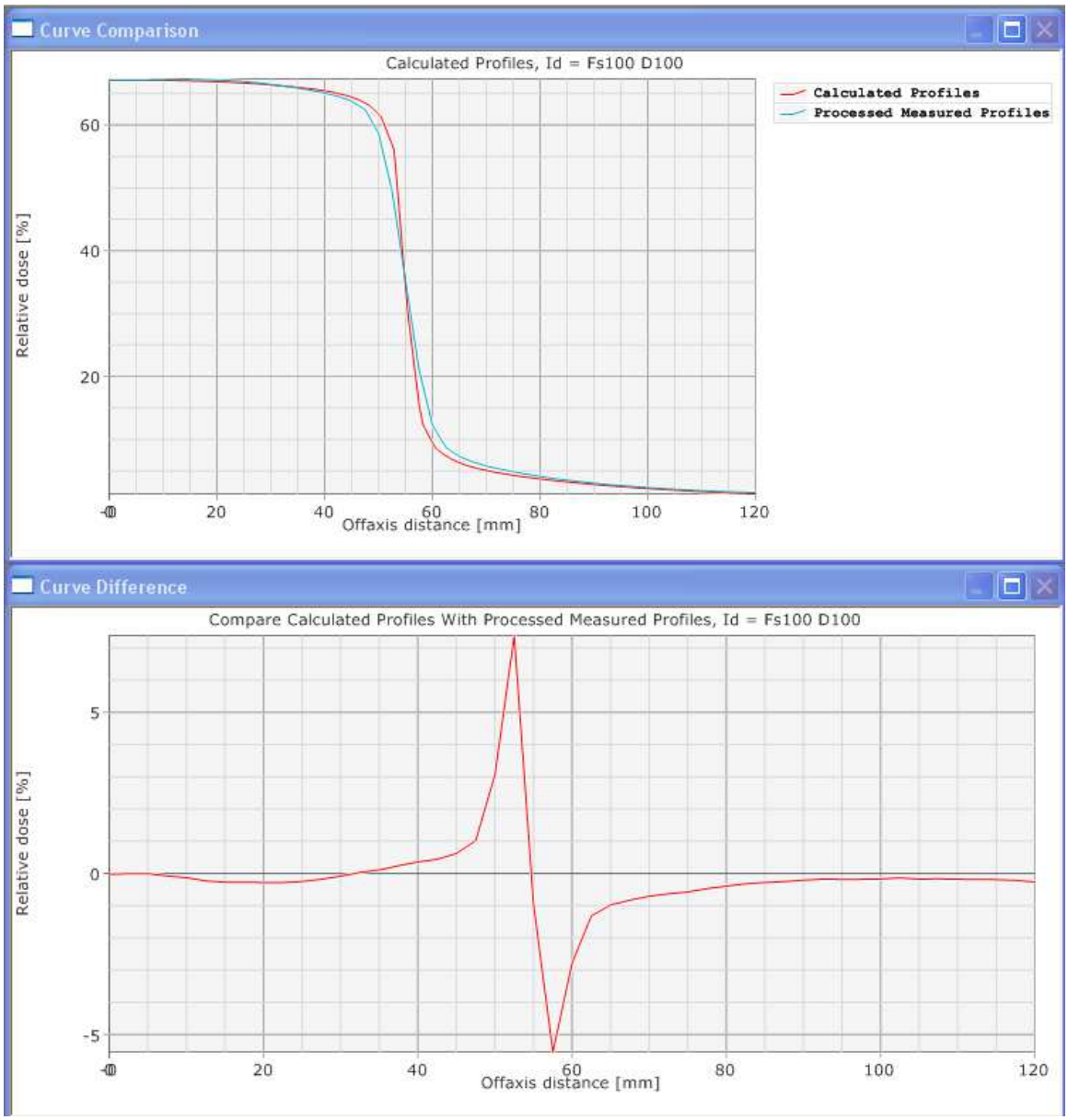


**Figure 3: Comparison of Original Calculated Beam Profile with no error and Measured Beam Profiles done in Verification.**

### 2.2.4 Dosimetric Leaf Gap and MLC Transmission Factor

The Dosimetric Leaf Gap and MLC Transmission Factor are not included in the dose calculation algorithm commissioning process. Values are input through the Beam Configuration window in Eclipse in the beam data tab under dosimetric data, which is done as a part of IMRT commissioning after the AAA beam modeling algorithm has been completed.

## *2.3 Implementation of Errors*

We introduced the following types of commissioning errors into the commissioning of the AAA beam modeling algorithm: alterations to MLC dosimetric leaf gap (MLC DLG), MLC transmission factor, flattening filter material, and electron contamination modeling parameters, input of Tissue-Maximum Ratio (TMR) as opposed to Percent Depth Dose (PDD) curves, and smoothing the input dose profiles to simulate measuring the beam data using an inappropriately large farmer chamber. When changes were made in the flattening filter material, the system would automatically modify second source parameters such as the size or mean energy of the second source. These automatic modifications are made to ensure that the calculated and measured dose curves match well, thus minimizing the clinical impact it would have if a mistake were made in entering the flattening filter material. While the system automatically

compensates for some errors by modifying other beam parameters, the AAA beam modeling system does not compensate for differences in MLC DLG.

The first type of error that was introduced was alterations in the Dosimetric Leaf Gap. The MLC DLG is a parameter used to model the complex interactions with a beam incident upon the leaves of a MLC such as lateral disequilibrium[6], tongue-and-groove effect, and rounded leaf-end effect. To account for these effects the dose calculation algorithm assumes a gap between the ends of leaf pairs. The magnitude of this gap is set by the physicist and can be determined by comparison of line profiles of delivered and calculated dose[7]. In our case, the original DLG was set to 1.8mm. We then implemented errors ranging from 0.1 to 1 mm from the nominal value.

Next, changes were made to the MLC Transmission Factor. The transmission factor models leakage dose through the MLC leaves. The transmission factor is determined using film measurements and determining the percentage of dose that is delivered to the blocked areas[19]. The original value of the MLC Transmission Factors as set in IMRT commissioning of this machine is 0.017, representing that 1.7% of the dose delivered is transmitted to areas blocked by the MLC leaves. We implemented changes in transmission factor of magnitude of 0.5% and 0.9% by changing this value to .022 and .026, respectively.

The next phase of commissioning errors implemented was the material of the flattening filter. The flattening filter is used in linear accelerators to preferentially

attenuate the beam at the center resulting in a beam hardening effect with the ultimate goal of achieving a flat dose profile at treatment depth. The AAA beam modeling algorithm allows the user to select the flattening filter material; we changed the material of the flattening filter from Copper to any of the other materials listed as possible flattening filters, which includes Tungsten, Lead and Iron. During the first step of the commissioning process machine parameters are input and using these parameters the TPS accesses a machine library that includes information about the specific machine that is being commissioned. To change the flattening filter from Copper to a different material, one must skip the step of the commissioning process that retrieves parameters from the machine library. Upon selecting an incorrect flattening filter material, the beam spectrum is altered. The AAA beam modeling algorithim then compensates for this by changing the second source parameters, resulting in close agreement between calculated and measured dose profiles and depth dose curves.

Another set of parameters retrieved from the machine library are the electron contamination parameters. Electron contamination fluence is simulated within the dose calculation algorithm using a convolution of aperture shape and a 2D sum-of-Gaussians kernel[1]. The parameters available for electron contamination are two different sigma values that model the lateral distribution for each Gaussian curve and a relative fraction specifying the weight of each Gaussian. The initial values from the machine library for $\sigma_0$ is 69.99 mm, $\sigma_1$ is 99.99 mm, and a relative fraction of 0.4384. The default

commissioning procedure will set these values automatically. To alter these values, the user must skip a step of the configuration process so that the values are not reset. For this project, changes were made in $\sigma_0$ of magnitude of 70 mm.

The next error implemented was to input TMR curves rather than PDD curves. Tissue Maximum Ratio, unlike Percent Depth Dose does not account for inverse square falloff and is simply a ratio of the dose at a given depth relative to the maximum dose given the same SAD for both measurements. Percent Depth Dose is also a ratio of dose but accounts for the change in distance from the source with depth. For input into the TPS, PDDs should be measured for the linear accelerator in water. To convert from PDD to TMR, a function in the beam data collection software was used for each field size and values at certain depths were verified by hand. Once TMR curves were input into the system instead of PDD curves, the commissioning process was carried out in its entirety.

The final error implemented was a smoothing of dose profiles to simulate the use of an inappropriately large farmer chamber while collecting the profiles. To do so, profiles were smoothed using an arithmetic mean smoothing method with a sliding window size of 6 mm in the beam data collection software. This sliding window size was used to simulate a large diameter chamber used to collect the data. These overly smoothed profiles were input to the TPS in place of the proper dose profiles and commissioning was carried out in its entirety. Figure 4 shows the smoothed profiles in blue and orange and the original, unsmoothed profiles in red and green.

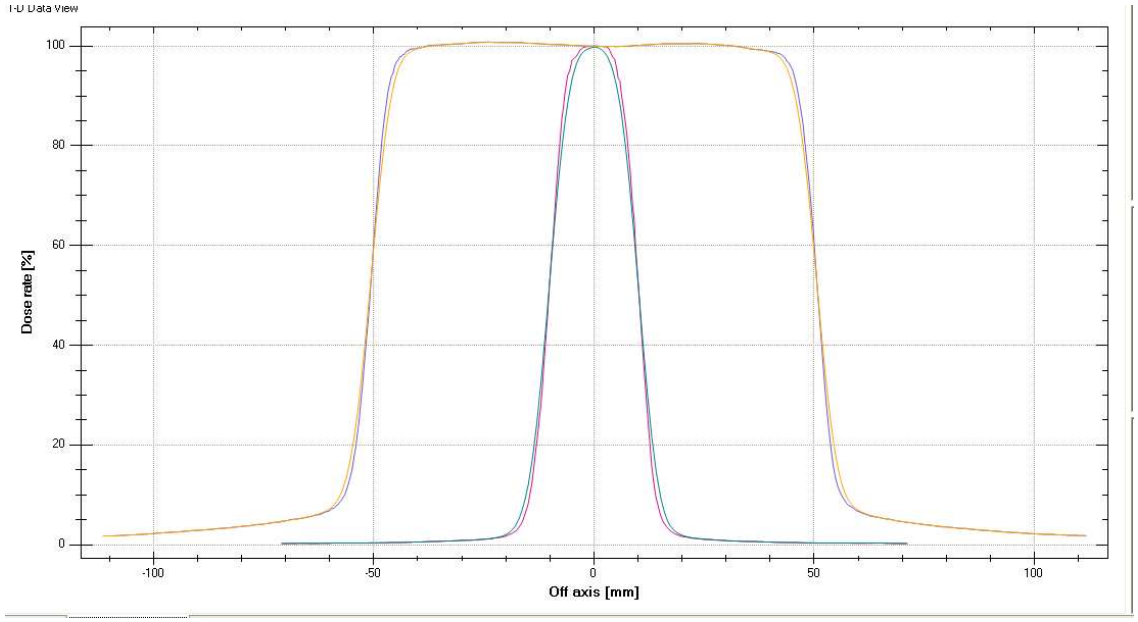


**Figure 4: Comparison of 6mm smoothed profiles to unsmoothed profiles for 2x2 cm and 10x10 cm field sizes.**

## *2.4 Clinical Impact*

To determine the clinical impact that these commissioning errors had, they were analyzed using standard dose metrics for five clinical plans. The plans used included a low risk prostate plan, an intermediate risk prostate plan, a head and neck plan, a Mesothelioma case, and a scalp case. Each of these plans has different source to surface distances (SSD), target volume sizes, and organs at risk near the treatment volume but all plans used a 6X beam for treatment. The variety allows us to examine how different errors would impact different clinical plans depending on these differences. The head and neck case and the scalp plan were the only plans used to analyze changes in electron contamination metrics as they were the only cases with critical structures within the electron range distance from the surface. To analyze the clinical impact of these errors,

we looked at d99 and d1 of the PTVs as well as mean or max dose statistics of nearby critical organs depending on if those organs were serial or parallel. The Mesothelioma case was used primarily to determine the effects of these errors in low dose regions. To quantify this, we considered the volume of the non treated lung to receive dose over 5 Gy, 13 Gy, and 30 Gy as well as the volume of the heart to receive over 38 Gy or 42 Gy. The prostate plans required the deepest penetration of any of the plans considered and were used in determining the impact of the implemented errors at depth. The original treatment plans are illustrated in Figures 5-9 as well as the Dose Volume Histograms showing the original dosimetric indices for each plan.

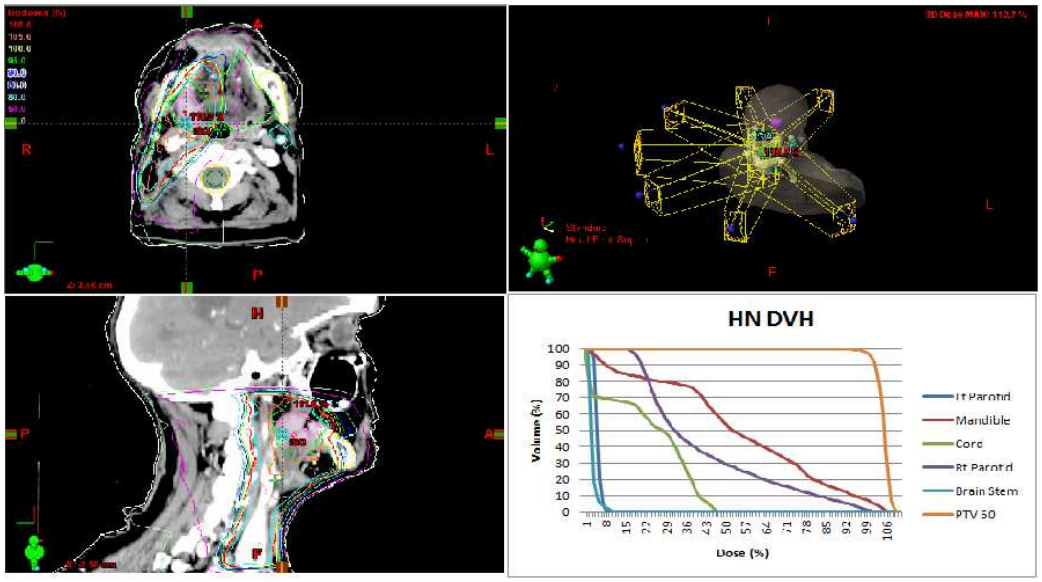


**Figure 5: 3D rendering, Axial, and Sagittal Dose Distribution and DVH of Head and Neck Plan.**

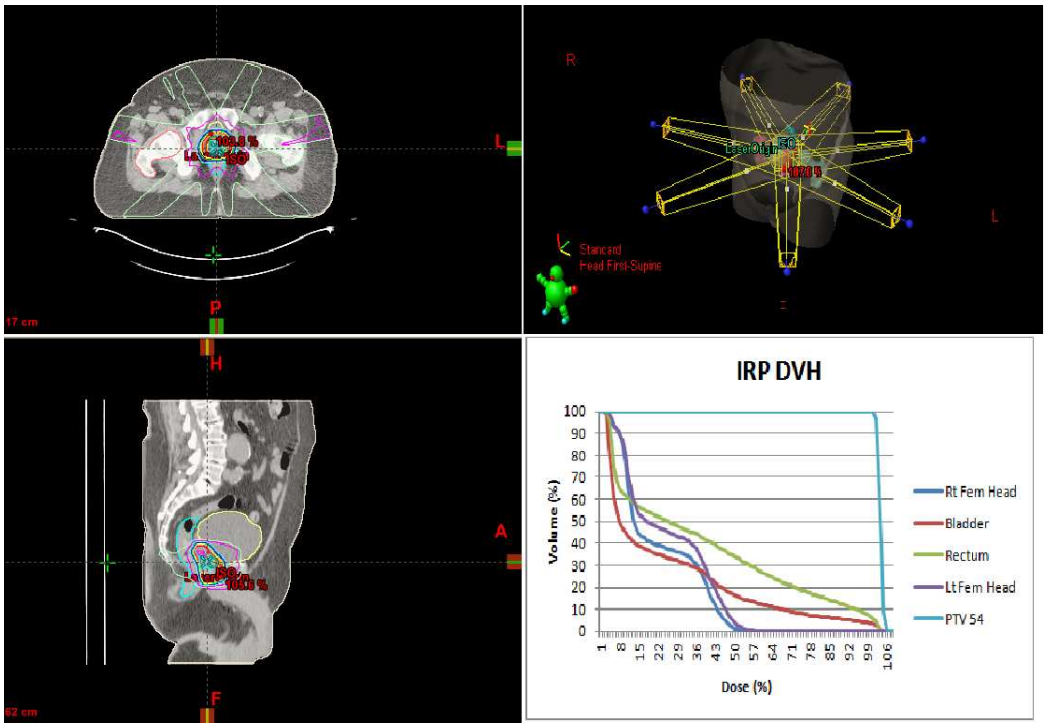


**Figure 6: 3D rendering, Axial, and Sagittal Dose Distribution and DVH of Intermediate Risk Prostate Plan.**

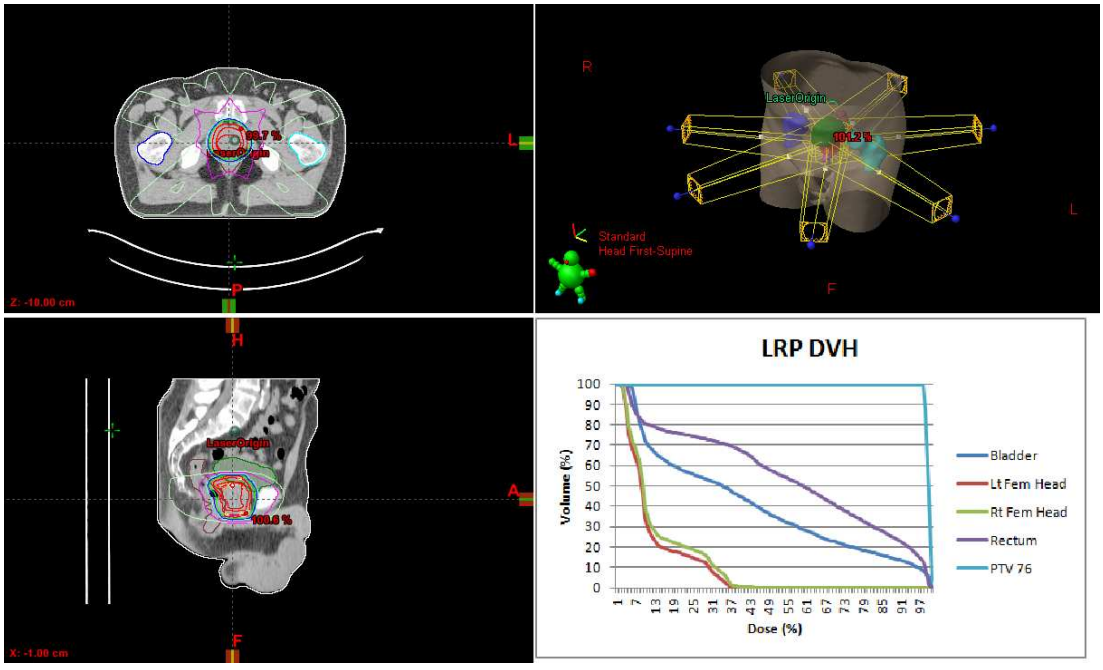


**Figure 7: 3D rendering, Axial, and Sagittal Dose Distribution and DVH of Low Risk Prostate Plan.**

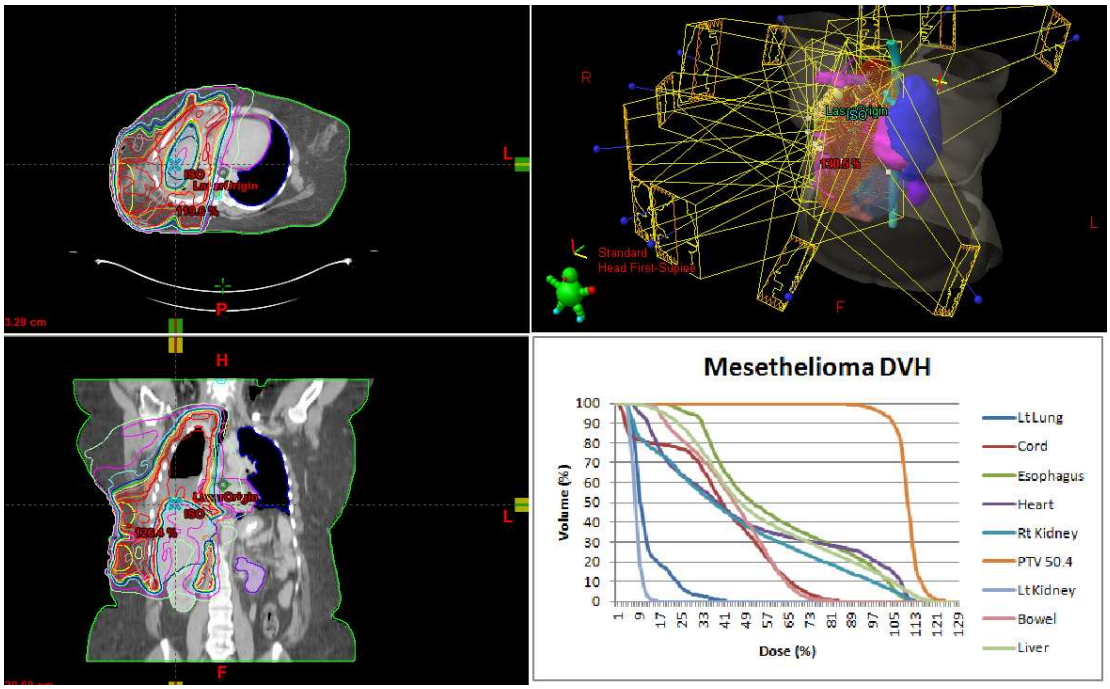


**Figure 8: 3D rendering, Axial, and Coronal Dose Distribution and DVH of Mesothelioma Plan.**

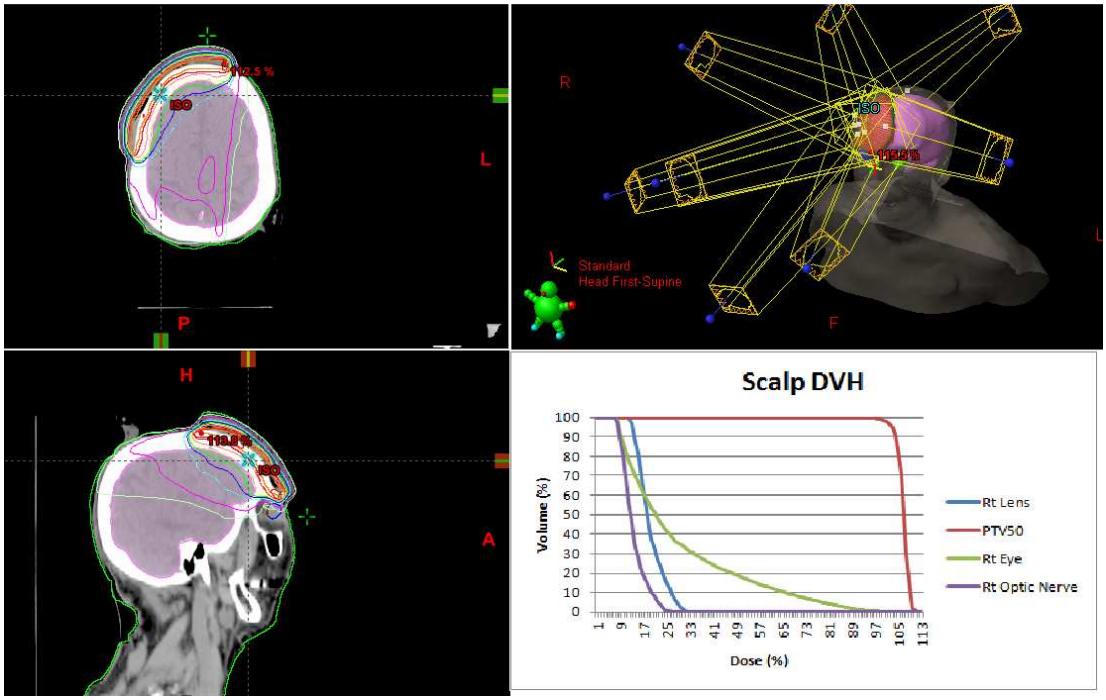


**Figure 9: 3D rendering, Axial, and Sagittal Dose Distribution and DVH of Scalp Plan.**

## 2.5 Sensitivity to Errors of IMRT Commissioning TG-119 Phantom

The sensitivity of the TG-119 IMRT commissioning process was evaluated by recalculating the dose distribution of a previously optimized plan using the altered AAA beam model. TG-119 gives two cases for C-shape phantoms, one that is easier to optimize with the central core structure receiving 50% of the prescribed dose, and a more difficult to optimize plan with the central core structure receiving only 20% of the prescribed dose. For this project the easier to optimize plan was used because we would expect this plan to be less sensitive to errors. The TG-119 C-shape phantom is assessed using three planar film measurements and evaluated using a two dimensional gamma analysis with the criteria of 3% dose 3mm distance to agreement. The three planes are shown in figure 10. When discussing the gamma analysis, the transverse plane shown in the top right will be referred to as the z plane, the coronal plane shown in the bottom left will be referred to as the y plane, and the sagittal plane shown in the bottom right will be referred to as the x plane.

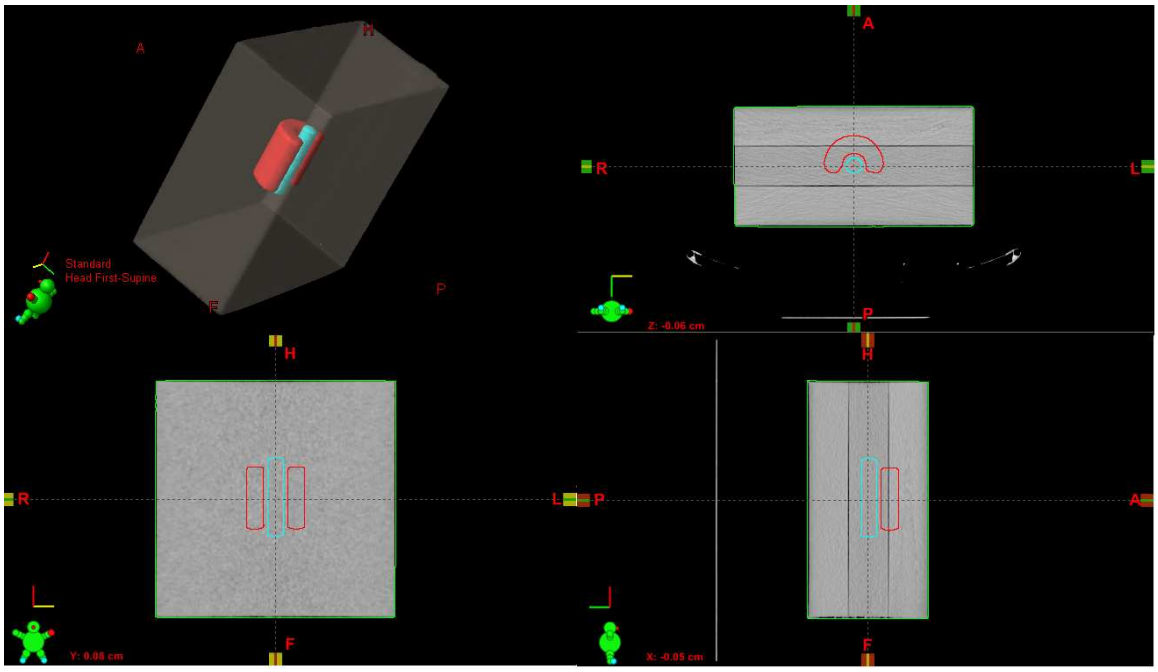


**Figure 10: 3D rendering and planar views of the TG-119 C-shape IMRT phantom.**

## 2.6 Sensitivity to Errors of IROC Credentialing

During the IROC credentialing process, the IROC analyzes the institution using point doses measured by eight TLDs within the IMRT head and neck phantom, four in the primary PTV, two in a secondary PTV, and two in the OAR, one superior and one inferior. To pass the IROC credentialing, the point dose measurements within the PTVs must be within 7% of the expected value. While all TLDs are measured, only the TLDs within the PTVs are considered during the IROC analysis. A sagittal film measurement is also measured and evaluated by the IROC using a 4mm distance to agreement metric for the midpoint dose between the PTV and OAR. The ability of IROC credentialing process to detect commissioning errors was tested by recalculating the dose distribution

of the plan administered to the respective phantoms using AAA after the changes had been made. Using the same criteria, we determined the discrepancy of errors introduced during commissioning.

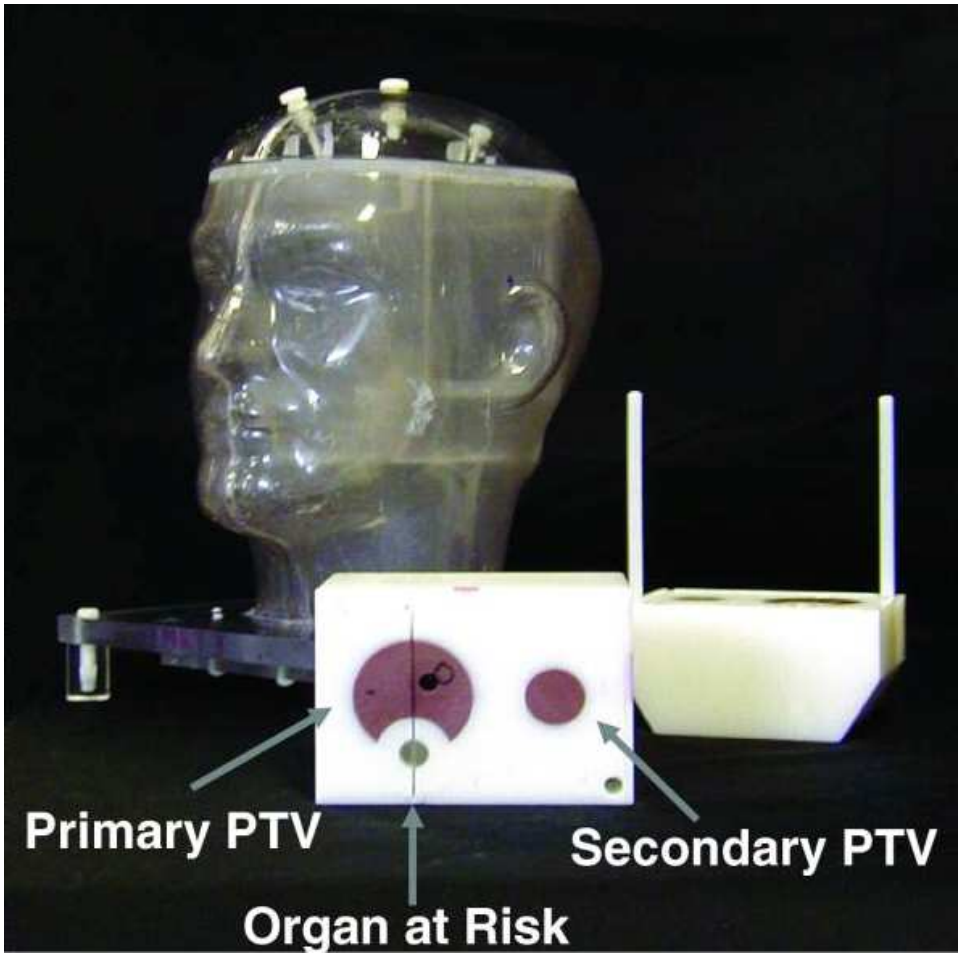


**Figure 11: IROC IMRT Head and Neck phantom. The Primary PTV is PT66, Secondary PTV in PTV54 and the Organ at Risk is the cord. The Sagittal film plane can be seen through the center of PTV66 and the cord.**

## 2.7 Potential Benefit of 3D dosimetry for TG-119 and IROC

The TG-119 commissioning process and the IROC credentialing processes use two dimensional film analysis and TLD measurements to evaluate the agreement between the IMRT calculation and delivery. In an attempt to evaluate the possible benefits of using 3D dosimetry in TG-119 commissioning and IROC credentialing, we calculated dose volumes for each plan with and without introducing commissioning errors. We then evaluated the change in relevant dosimetric indices based on the contoured organs at risk taken from the dose volume constraints of the plan. We determined the sensitivity of these indices from the 3D dose distributions to commissioning errors and compared it to the sensitivity of the current 2D practices used in TG-119 and IROC credentialing.

# 3 Results

## *3.1 Overview*

Table 3 summarizes the clinical severity of the various commissioning errors and probability of the errors being detected by the treatment planning system during dose calculation algorithm preparation stage. It also includes the probability of their being detected during commissioning following the TG 119 guidelines and during credentialing through the IROC. Clinical severity and detection probability were graded as low, medium, or high based upon our results. For clinical severity and TLD detection Low was given if the effect was less than 2%, Mid if the effect was between 2% and 7%, and High if the effect was greater than 7% which would fail the IROC credentialing criteria for the TLD measurements. The ability of the TPS to detect errors was graded as High when the system gave a visual warning and did not allow the user to continue, was graded as Mid if the error could be detected visually during the verification stage but no warning was given, and Low if there was no indication from the TPS that an error occurred. The clinical severity of Electron Contamination errors was ranked as Low-Mid because it only had a non-negligible (2.1%) effect on one of the five clinical plans analyzed (the scalp plan). A Low-Mid ranking was also assigned to the ability of TPS to detect flattening filter material errors as a step of the commissioning process in which parameters are retrieved from the machine library must be skipped for the error to be implemented.

**Table 3: Summary of clinical severity and probability of detection for errors implemented in Eclipse AAA.**

| Type of Error | Clinical Severity | Ability of TPS to detect | IROC PTV TLDs | IROC OAR TLDs | IROC film | TG 119 Absolute | TG-119 Relative | 3D Dosimetry IROC | 3D Dosimetry TG-119 |
|---|---|---|---|---|---|---|---|---|---|
| MLC DLG .5 mm | Mid | Low | Mid | Mid | Low | Mid | Low | High | Mid |
| MLC DLG 1 mm | High | Low | High | High | Low | High | Mid | High | High |
| Transmission Factor 0.5% | Mid | Low | Low | Mid | Low | Low | Low | Mid | Mid |
| Transmission Factor 0.9% | High | Low | Mid | High | Low | Low | Mid | Mid | Mid |
| FF material | Low | Low-Mid | Low | High | Low | Low | Low | Low | Low |
| Smoothed for farmer chamber | Low | Mid | Low | Low | Low | Low | Low | Low | Low |
| TMR vs. PDD | High | Mid | High | High | Mid | High | Low | High | High |
| SAD | High | High | N/A | N/A | N/A | N/A | N/A | N/A | N/A |
| Electron Contamination | Low-Mid | Mid | Low | Low | Low | Low | Low | Low | Low |

## *3.2 Clinical Impact*

### 3.2.1 Dosimetric Leaf Gap

Because MLC DLG is input apart from the AAA beam modeling algorithm, errors in the DLG were the least likely to be detected by the TPS. The input of an incorrect DLG was straightforward and the effects of input of an improper DLG value was undetectable looking at the comparison between calculated and measured dose profiles during verification. As shown in Figures 12, 13, and 14, the relationship between the magnitude of change in the DLG value is proportional to the dosimetric effect induced by the error. Interestingly, the slope of correspondence between the magnitude of error and dosimetric effect varies between organs. The most sensitive organs to changes in the DLG are the parotid glands, in which a 2% dosimetric effect occurs with a change in DLG of 0.2 mm and a 5% dosimetric effect with a change of 0.5 mm. Prostate plans however were less sensitive to changes made in DLG values with all dosimetric indices remaining within 2% for 0.5 mm changes. This is true for the PTVs of all plans, with the only dosimetric indices outside of 2% being the lens and optic nerve in the scalp case.

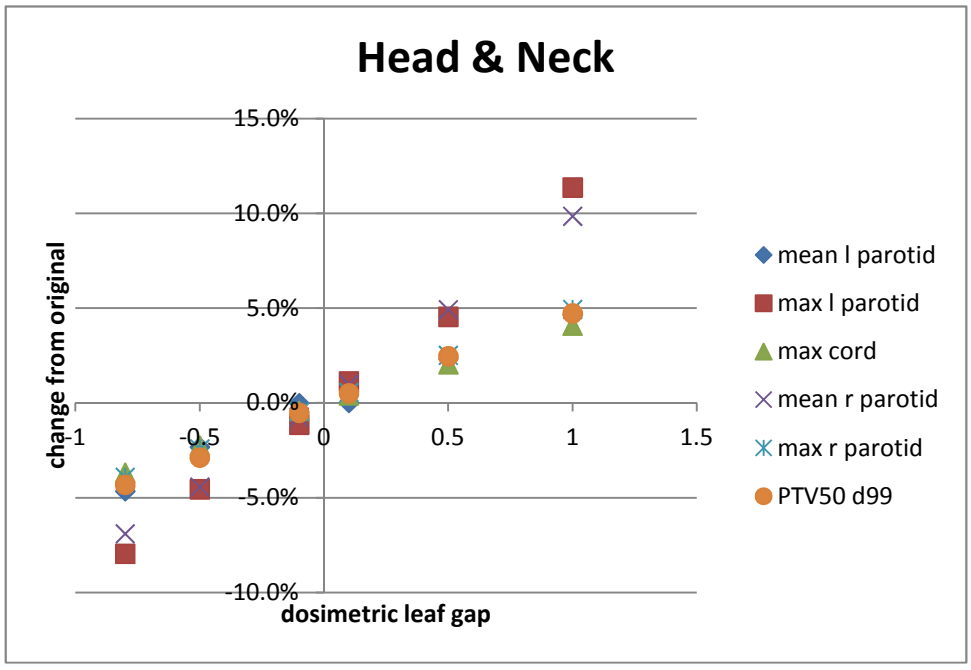


**Figure 12: Display of change in dose from original Head and Neck plan with changes in the MLC DLG.**

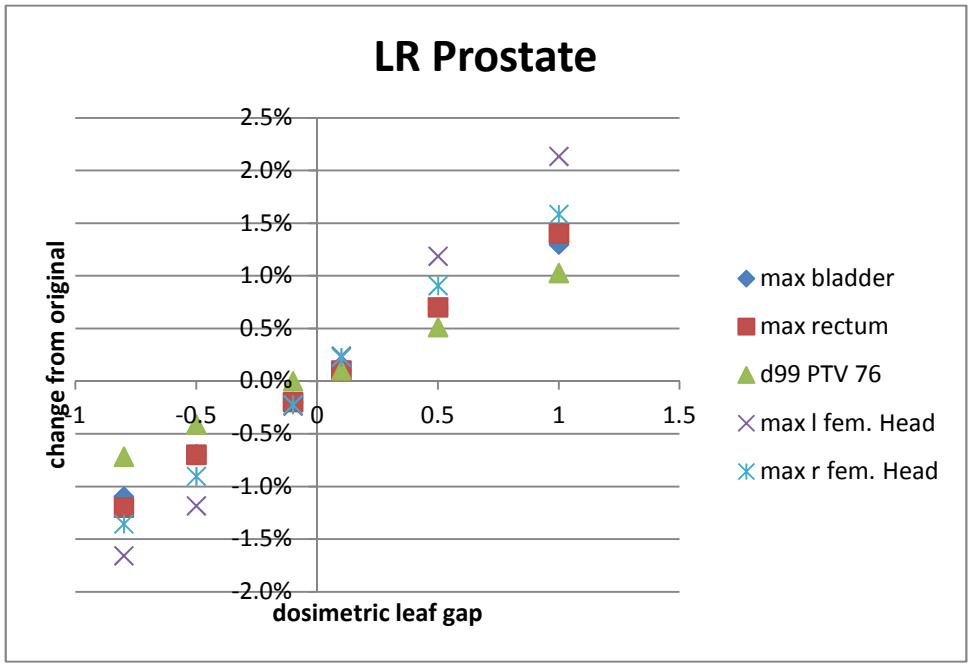


**Figure 13: Display of change in dose from the original LR prostate plan with changes in the MLC DLG.**

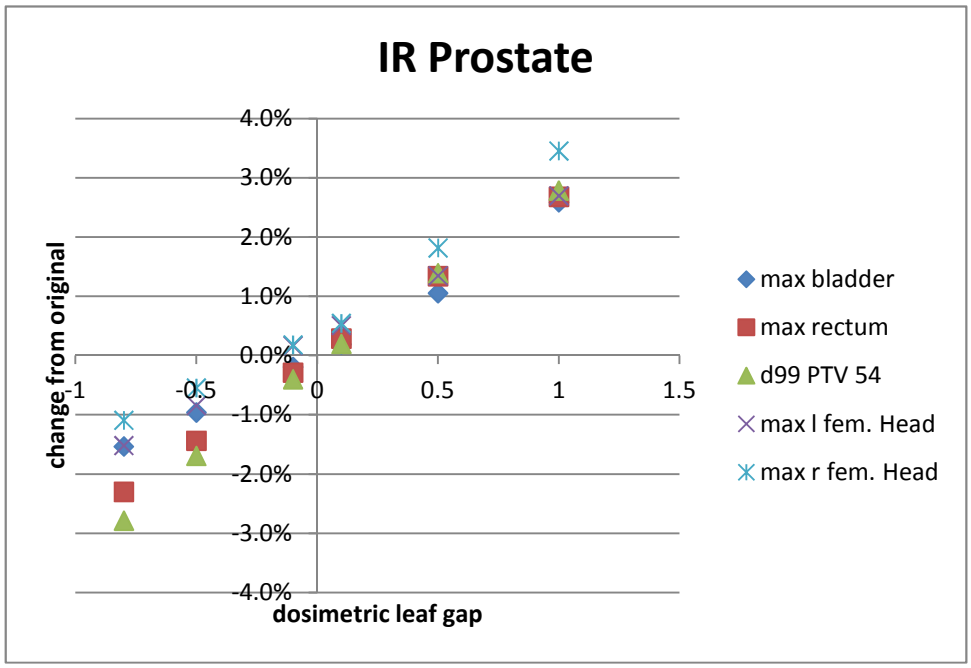


**Figure 14: Display of change in dose from original IR prostate plan with changes in the MLC DLG.**

### 3.2.2 MLC Transmission Factor

Making changes to the MLC transmission factor value was also done apart from the AAA beam modeling algorithm and was undetectable in the verification stage of the TPS commissioning process. Similarly to DLG errors, the magnitude of changes in transmission factor was proportional to the dosimetric effect induced by the error. The most sensitive plans to transmission factor errors were the head and neck plan and scalp plan. In the head and neck plan a 0.9% change in transmission factor resulted in a 7% change to the mean dose to the right parotid and a 0.5% change in transmission factor resulted in a 4% change to the mean dose to the right parotid. In the scalp plan a 0.9% change in transmission factor resulted in an 8% difference in the maximum dose to the

right optic nerve and a 0.5% change in transmission factor resulted in a 5% change in the maximum dose to the right optic nerve. The prostate and lung plans were less sensitive, with these same changes in transmission factor resulting in changes of less than 2% in relevant dosimetric indices.

### 3.2.3 Flattening Filter Material

The TPS was more sensitive to detecting changes made in flattening filter material in that it would reset the flattening filter material to the proper value when retrieving parameters from the machine library. If the user manually overrode the retrieval from the machine parameter library, the AAA beam modeling algorithm still compensated for the incorrect flattening filter setting by changing other parameters, specifically size, relative intensity and mean energy of the second source. As a result, the beam model matched the input profiles with the exception of the penumbra region where 5% differences occurred. The clinical impact of changing the flattening filter in the TPS was minor in all of the plans considered, resulting in a mean change of within 0.3% in all of the clinical plans and a maximum change of 2.3% in the parotids in the head and neck plan which is a very low dose region that receives less than 9% of the prescription dose.

### 3.2.4 Inappropriately large farmer chamber

Implementation of an inappropriately smoothed dose profiles went relatively undetected by the TPS. Similarly to the incorrect flattening filter material, differences

could be detected within the TPS during the verification process by looking at the penumbra of the dose profiles where there was up to a 10% difference in the penumbra region. In general the clinical effect was minimal and within fractions of a percent, with the exception of the V20 in the untreated left lung in the Mesothelioma case which saw a change of more than 6% its original value. The effect of smoothing was minimized within the TPS because the calculated profiles matched the actual profiles better than they matched the input (smoothed) profiles. While the AAA beam modeling algorithm attempts to match the calculation with the measured profiles, the differences detected between the two near the penumbra show that the TPS partially corrected the user error and decreased the effect that using an inappropriately large farmer chamber would have on the dose calculation algorithm.

### 3.2.5 TMR

Clinically, input of TMR instead of PDD was the most severe of the errors made during the commissioning process. TMR errors had large clinical impact, with a mean difference in dosimetric indices of over 13% in prostate plans. All plans had changes in some dosimetric indices of over 5% with the least sensitive plan being the scalp case. This is unsurprising as the scalp case consists mainly of dosimetric indices near the surface and the largest discrepancies between TMR and PDD occurs at deeper depths. Figure 15 shows a comparison of planar dose distributions for the original and TMR calculated intermediate risk prostate plan.

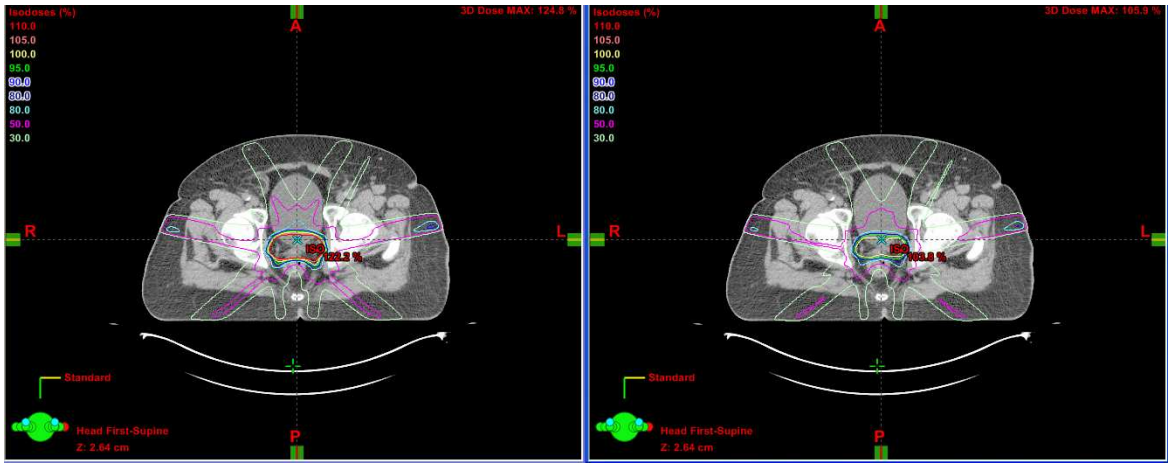


**Figure 15: Comparison of isodose distributions for the original Intermediate Risk Prostate plan (right) compared to TMR (left).**

### 3.2.6 Electron Contamination

Electron contamination was the most difficult error to implement into the system. The TPS normally retrieves the electron contamination parameters from the machine library, so to make any alterations to the parameters requires that the user prevent the TPS from searching in the machine library. After the user skips this step and makes a change to the parameters, the user must skip the second step of the configuration process to prevent the value from being changed back to their original values. It therefore requires that multiple errors be made by the user, or alternatively that the values retrieved from the library be corrupted. Upon calculation of the percent depth dose curves and dose profiles, the user can then see a notable difference of up to 20% in the surface dose in the PDD for changes of 70 mm in $\sigma_0$. The only plan that saw any considerable dosimetric effect was the scalp case with a maximum dose difference of over 2% in the mean dose to the right lens. Hence the AAA beam modeling algorithm

within the Eclipse TPS is very robust and resistant to electron contamination errors as they require multiple errors and input of values very far from the original values, and there is only a clinical effect of such errors for a PTV or OARs neat the skin surface.

### 3.2.7 SSD changes

Changes to the source to surface distance are expected to have a very large dosimetric effect if they were to be implemented. However; the system prohibited the user to enter an incorrect SSD giving the error "Internal Error occurred in analyzing basic beam measurement data". The user was prevented by the TPS from proceeding without correcting the error.

## *3.3 TG-119*

TG119 C-shape phantom was relatively ineffective at detecting errors using analysis of dose statistics and distance to agreement test of planar films. For the DLG changes, the gamma pass rates varied as one would expect, with high pass rates for the small changes that had small dosimetric effects and lower pass rates for the larger changes that had more severe dosimetric effects. Figure shows the current effectiveness of TG-119 film analysis at detecting errors along with the potential for improved sensitivity by changing the gamma analysis metric from 3% 3mm to 2% 2mm. The vertical lines in Figure represent the DLG error from which we could see a clinical difference of 2% and 5% respectively. Using the current 3% 3mm gamma criteria, these

errors are within the standard deviation of pass rates among treatment centers that submitted their results[4].

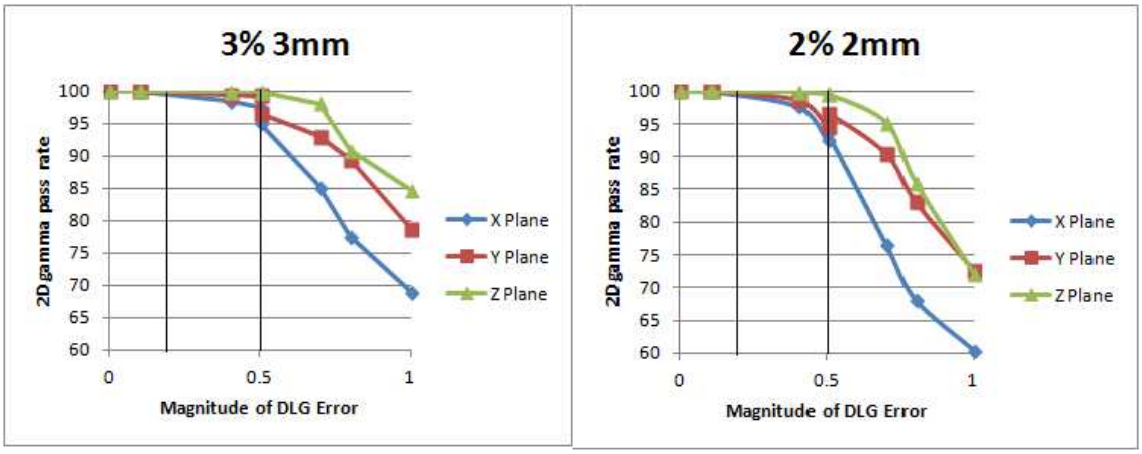


**Figure 16: Effectiveness of TG-119 at detecting Dosimetric Leaf Gap errors and TMR input.**

For changes in flattening filter material as well as over smoothing of dose profiles, TG-119 did not detect any errors and all of the different materials had pass rates of 100% in all planes. Since the dosimetric effect of these errors was minimal it is not surprising that TG-119 would have difficulty detecting any difference. Large changes in electron contamination parameters went undetected by TG-119 film analysis as all three planes had pass rates of 100%.

**Table 4: Pass Rates for various gamma criteria for each error in TG-119 film planes.**

| Type of Error | 3% 3mm Absolute gamma analysis | 2% 2mm Absolute gamma analysis | 3% 3mm Relative gamma analysis |
|---|---|---|---|
| MLC DLG .5 mm | 98.03 ± 1.96 % | 96.17 ± 1.96 % | 100 ± 0 % |
| MLC DLG 1 mm | 77.43 ± 7.97 % | 68.4 ± 6.84 % | 93.07 ± 8.22 % |
| Transmission Factor 0.5% change | 95.89 ± 3.55 % | 95.05 ± 4.05 % | 97.33 ± 2.29 % |
| Transmission Factor 0.9% change | 92.02 ± 5.16% | 88.72 ± 6.49 % | 95.15 ± 3.92 % |
| Incorrect FF material | 100 ± 0 % | 100 ± 0 % | 100 ± 0 % |
| Smoothed for farmer chamber | 100 ± 0 % | 100 ± 0 % | 100 ± 0 % |
| TMR vs. PDD | **53.37 ± 6.10 %** | **44.97 ± 4.19 %** | **98.13 ± 2.34 %** |
| Electron Contamination | 100 ± 0 % | 100 ± 0 % | 100 ± 0 % |

The most easily detected error was the input of TMR instead of PDD, which was expected as it had the largest dosimetric effect in the clinical plans with pass rates below 50% for an absolute gamma analysis with criteria of 3% 3mm. However, when analyzed using a relative gamma comparison in which both the original and the TMR planes were normalized to their maximum values the pass rates were better than 95% for all planes. The same was true for DLG errors analyzed with relative gamma analysis for which a 0.5 mm change in DLG went completely undetected with a 100% pass rate. This emphasizes the need for an absolute rather than relative dose comparison, as a relative

comparison can miss even drastic commissioning errors, as shown both in table 5 and figure 17.

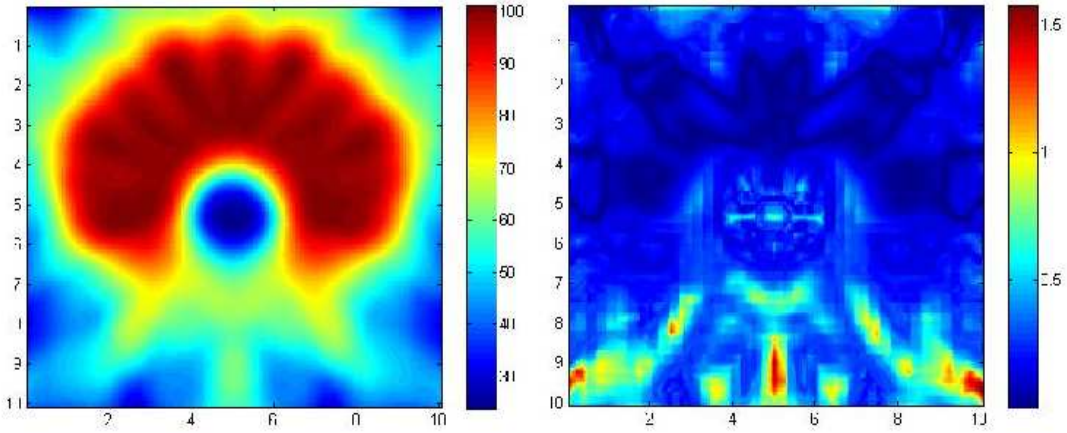

**Figure 17: Original Axial Dose Plane (Left) and Relative Gamma Map (right) for TMR comparison with the TG-119 C-shape phantom. This relative gamma analysis was done with a criteria of 3%, 3mm and had a pass rate of 95%.**

## *3.4 IROC*

Figures 18 and 19 show the sensitivity of IROC TLDs to various commissioning errors. While the PTV TLDs were effective in detecting clinically relevant errors such as the DLG errors as shown in Figure 18, Figure 19 shows that the OAR TLDs are much more efficient in detecting errors in flattening filter material and MLC transmission factor.

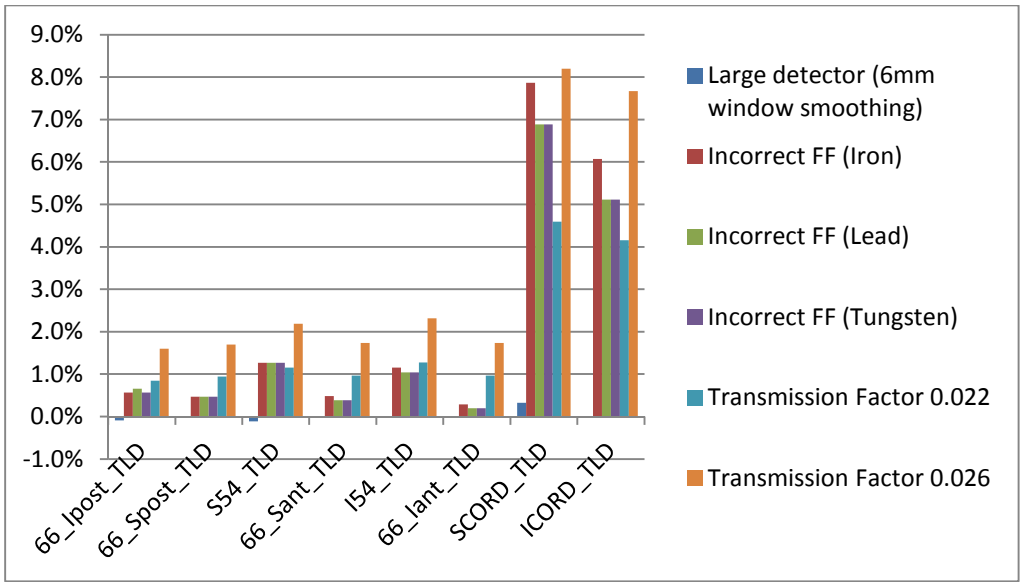


**Figure 18: Sensitivity of point dose measurement to flattening filter, smoothing changes, and transmission factor changes in IROC IMRT phantom.**

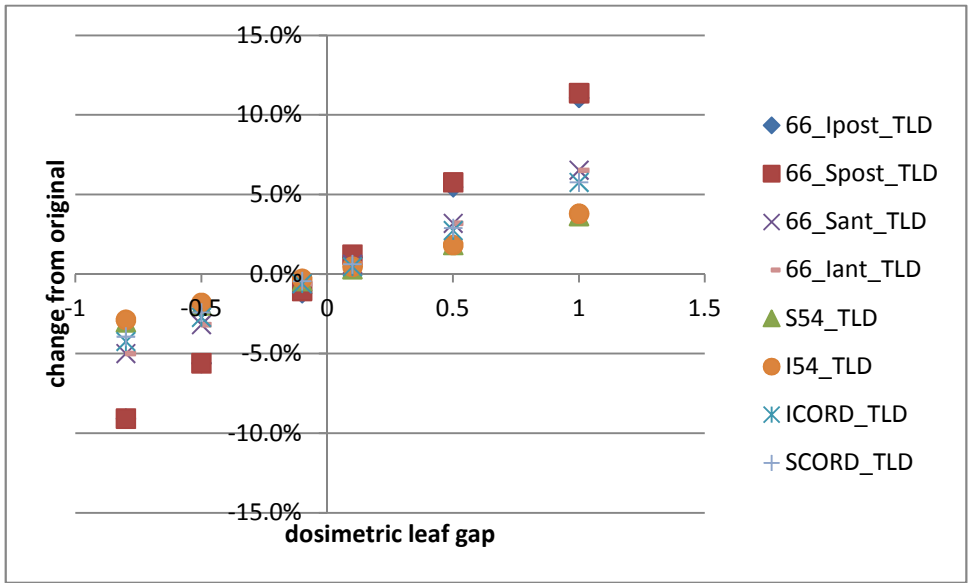


**Figure 19: Sensitivity of point does measurement to dosimetric leaf gap changes in IROC IMRT phantom.**

IROC TLD measurements were effective in detecting TMR errors as there was a mean difference of 10% between the original plan and the TMR plan.

The sagittal film planes were analyzed and the only error that did not meet the 4 mm distance to agreement criteria was the TMR error which had a distance to agreement of 6mm. All DLG errors, flattening filter errors, and profile smoothing each fell well within the 4 mm criteria with no distance to agreement greater than 1mm.

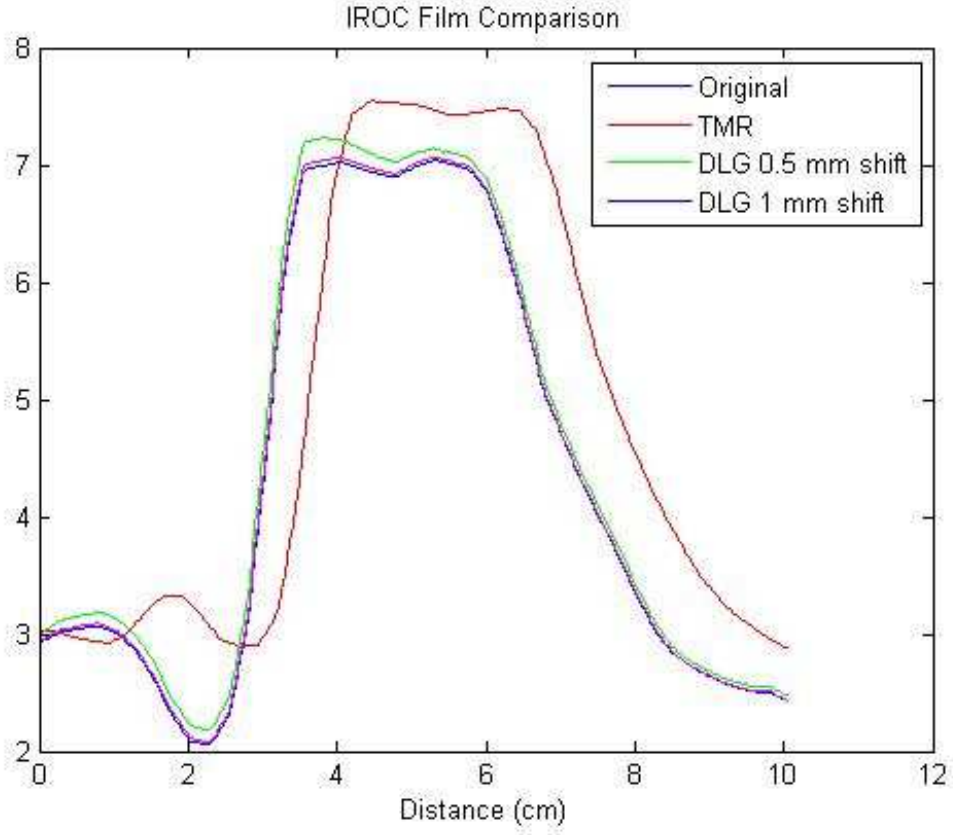


**Figure 20 : Sample of IROC film comparison analyzed with distance to agreement metric of 4mm.**

## 3.5 3D Dosimetry

3D dosimetry analysis of the TG-119 C-shape phantom proved to be very sensitive to DLG errors, specifically with OAR indices changing more than 6% for a 0.5 mm change and more than 14% for changes of 1 mm as shown in Figure 21. Figure 23 shows the sensitivity of 3D dosimetric indices in the TG-119 C-shape phantom to flattening filter and smoothing errors, which while they did show a difference were so small in magnitude that they would not be detectable.

3D dosimetric analysis as applied to the IROC IMRT head and neck phantom was also sensitive to DLG errors with the cord as the most sensitive dosimetric index to errors. The max dose to the cord changed by over 6% for a 0.5 mm shift and over 13% for a 1 mm difference as shown in Figure 24.

3D dosimetry proved to have advantages over the 2D techniques currently used in TG-119 commissioning. Absolute 2D gamma analysis as recommended by TG-119 is relatively insensitive to DLG errors with 0.5 mm shifts still within the standard deviation of treatment centers that submitted data. Relative gamma analysis was minimally sensitive to all errors, with TMR errors passing at a 99% rate and 0.8 mm DLG shifts passing at a 100% rate. 3D dosimetric analysis was very sensitive to TMR errors, with over a 10% difference in all 3D dosimetric indices considered. The difference in sensitivity between 3D dosimetric analysis and relative gamma analysis is shown between Figures 17 and 22.

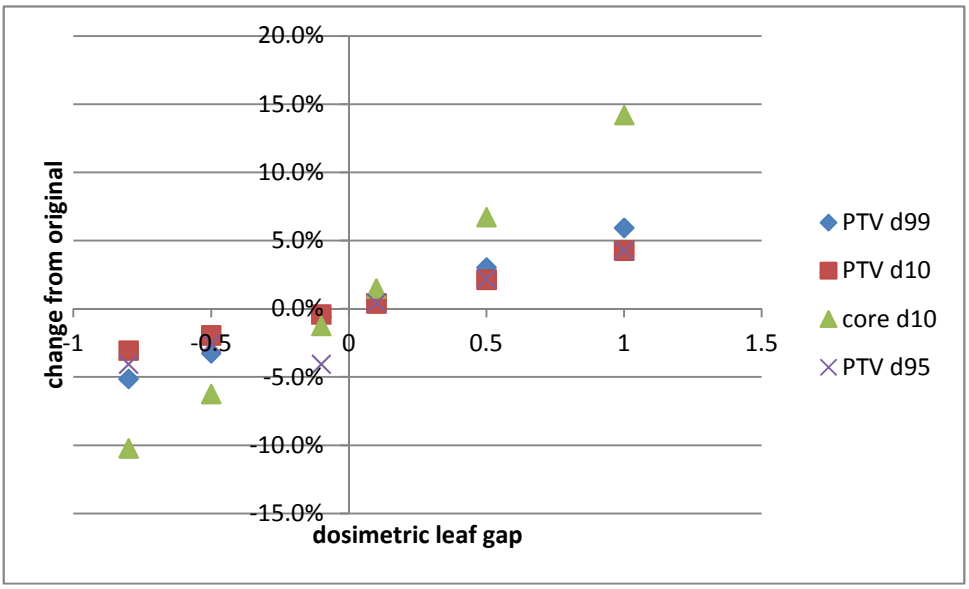


**Figure 21: Sensitivity of 3D dosimetric indices to DLG errors.**

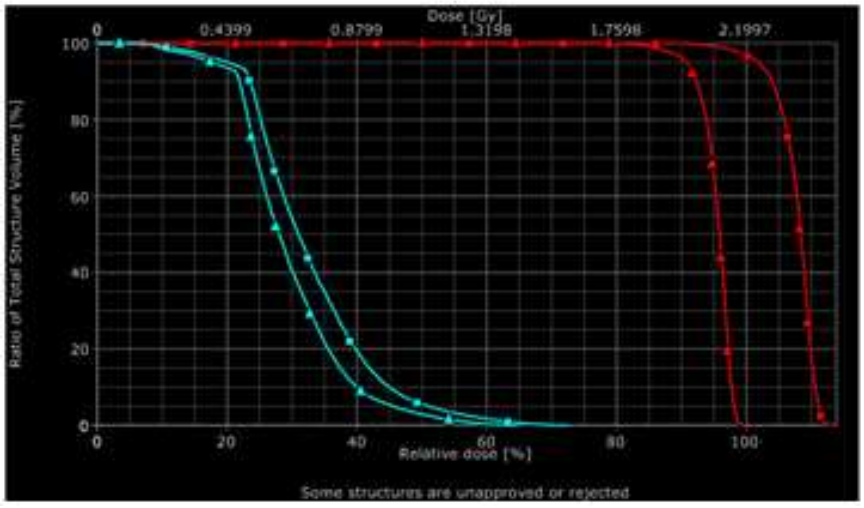


**Figure 22: DVH comparison for TG-119 C-shape plan between the original plan (triangles) and TMR plan (squares). The core OAR is shown in blue and the PTV is in red.**

While the 2D film analysis used in TG-119 was not able to detect any difference when incorrect flattening filters were used in commissioning, there were small changes that could be seen with the 3D dosimetric indices. The same is true for inappropriately

large detector being used during the collection of beam data. While these differences were detected more with 3D indices than gamma analysis, the effects of the errors were negligible.

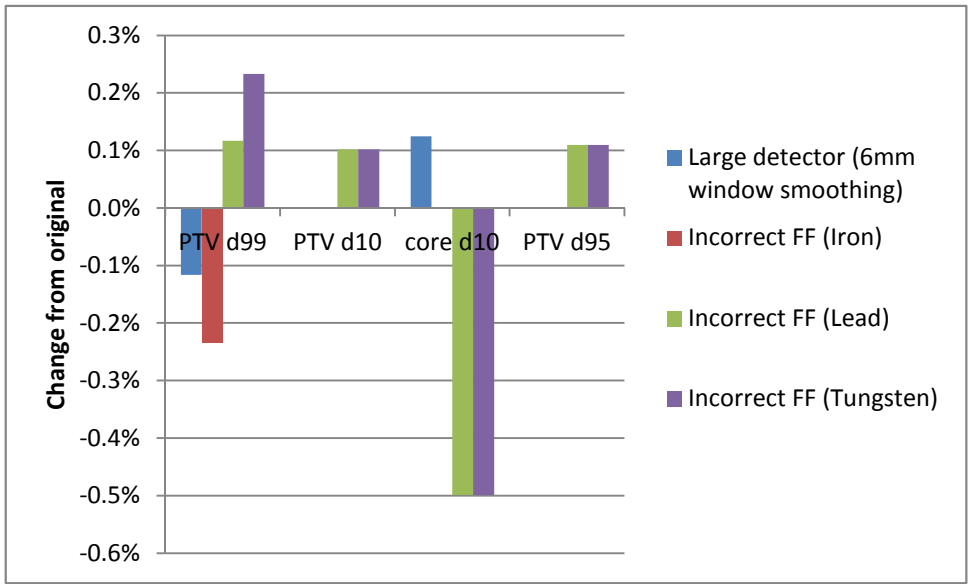


**Figure 23: Sensitivity of 3D dosimetric indices in TG-119.**

The current IROC credentialing procedures are very close in sensitivity to those that could be implemented with 3D dosimetry. Figure 23 shows the sensitivity of some 3D dose indices to changes in DLG. For changes in DLG, 3D dose indices are equally sensitive to the IROC TLDs with a 2% difference noticed with a 0.2 mm shift and a 5% difference noticed with a 0.5 mm shift. The same is true for TMR input for which the TLDs had a mean difference of 9.85% and the 3D dose indices had a maximum difference of 10.95%. Similarly to the TLD measurements where the OAR TLDs were more sensitive than the PTV TLDs to all errors, 3D dosimetric indices were most sensitive in low dose regions. Figure 25 shows the sensitivity of each clinical plan

considered and each detection method used by measuring the slope of plots of percent change in dosimetric indices versus change in DLG value.

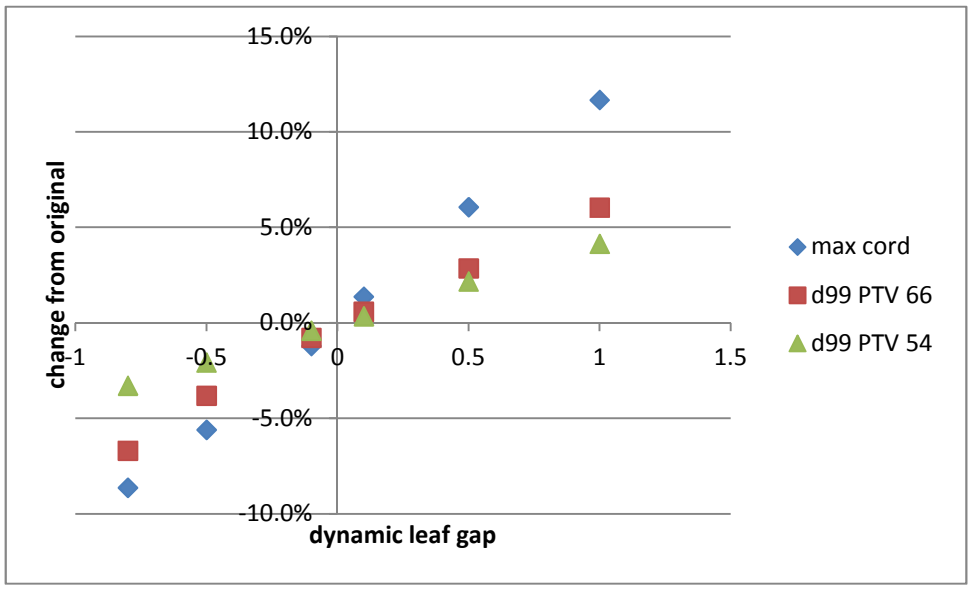


**Figure 24: Sensitivity of 3D dosimetric indices in IROC phantom.**

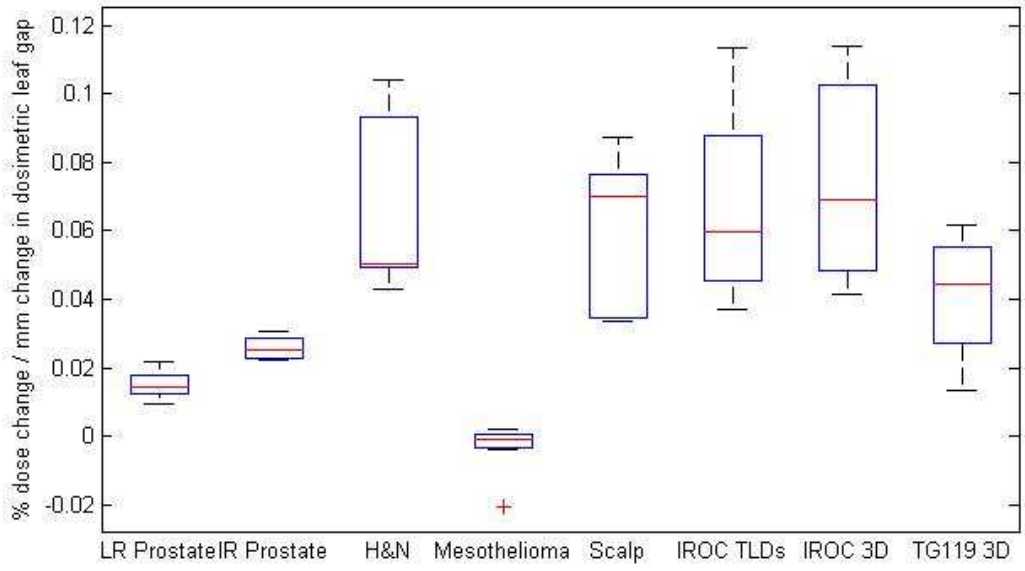


**Figure 25 : Sensitivity of clinical cases and detection methods for DLG errors.**

# 4 Discussion

In our observation, the AAA was robust at preventing errors from being implemented. Many errors were prohibited by the TPS because it was able to detect that the input parameters were incorrect (in the case of second source parameters), or geometrically impossible (in the case of SSD changes). Beyond not allowing certain changes, the AAA commissioning process was able to correct user error by altering other parameters in many cases and fitting the calculated beam modeling data to fit the measured beam data. For example, in implementing incorrect flattening filter material, the machine recalculated parameters including the size of second source, mean energy of second source, and relative energy of the second source to compensate for the incorrect energy spectrum resulting from the wrong flattening filter material. These alteration made by the machine shaped the calculated dose profiles and depth dose curves to more accurately match the measured dose profiles and depth dose curves input by the user that had the copper flattening filter. By altering these second source parameters, the spectrum was corrected so that the calculated and measured curves matched within 5% at all points throughout the curves. In the case of the overly smoothed dose profiles the calculated profiles matched the actual beam profile better than the smoothed profile along the penumbra.

In the IROC credentialing, TLD point does measurements along the critical structure meant to be avoided are measured but not analyzed. In our data these TLDs were the most sensitive to detecting certain commissioning errors. Our results indicate that these measurements may be useful to include in credentialing as they were the most sensitive overall to errors. However, the OAR TLDs were overly sensitive to errors that clinically had minor effects. 3D dosimetric indices were generally better correlated to the clinical severity of the errors implemented. In order to detect the errors in electron contamination parameters or MLC transmission factor, dose measurements would need to be made in low dose regions and, in the case of electron contamination, near the surface.

Recently, an effort has been made to failure mode and effects analysis (FMEA) to the field of radiation therapy as a means of reviewing the many components of the treatment process that could go wrong[2]. FMEA is a primarily qualitative analysis of a complex system that is a systematic technique for failure analysis. It involves three steps: (1) the probability that a specific cause will results in a failure mode. (2) The severity of the effects of a failure mode should it go undetected. And (3) the probability that the failure mode resulting from the specific cause would go undetected. It is able to account for each possible cause of failure in a system and if applied to IMRT could serve as an effective means of identifying the cause of failures or errors depending on their probability of occurrence and probability of detection at each step of the process[2]. Our

results have implications for this process, specifically table 2 and may be useful when assessing severity and probability of various commissioning errors. In table 2, the 'Ability for TPS to detect' column addresses the probability of an error occurring. The 'Clinical Severity' column addresses the clinical relevance of each error and the IROC and TG-119 columns address the probability of the errors being detected after the fact with the current commissioning guidelines and credentialing procedures in place. The 3D Dosimetry columns then assess the possible sensitivity of the current procedures if 3D dosimetric indices were used rather than planar and point dose measurements.

# 5 Conclusion

The AAA commissioning process within the Eclipse TPS is surprisingly robust to user error. The most severe of errors implemented was the input of TMR curve as opposed to PDD. While this error had severe clinical effects, it was easily detected with IROC credentialing and TG 119 commissioning. No commissioning errors were found to have both a low detection probability and high clinical severity. When errors do occur, the IROC credentialing and TG 119 commissioning criteria are generally effective at detecting them; however OAR TLDs are the most sensitive despite the IROC currently excluding them from analysis. IROC film analysis was ineffective in detecting the commissioning errors that we implemented. 3D dosimetry is more sensitive than the current 2D planar comparisons at detecting errors made in commissioning the dose calculation algorithm especially in the low dose region, but is roughly equivalently sensitive to the TLD point dose measurements currently done in IROC credentialing. It is also critically necessary to do absolute dose plane comparison rather than relative comparison, as relative gamma analysis was unable to detect even the most dramatic of commissioning errors.

# References


1) Eclipse Algorithms Reference Guide. Palo Alto, CA; 2007. Varian Medical Systems, Inc.

2) Huq, M. Saiful, Benedick A. Fraass, Peter B. Dunscombe, John P. Gibbons, Geoffrey S. Ibbott, Paul M. Medin, Arno Mundt, Sassa Mutic, Jatinder R. Palta, Bruce R. Thomadsen, Jeffrey F. Williamson, and Ellen D. Yorke. "A Method for Evaluating Quality Assurance Needs in Radiation Therapy." *International Journal of Radiation Oncology*Biology*Physics* 71.1 (2008): S170-173.

3) Fraass, Benedick, Karen Doppke, Margie Hunt, Gerald Kutcher, George Starkschall, Robin Stern, and Jake Van Dyke. "American Association of Physicists in Medicine Radiation Therapy Committee Task Group 53: Quality Assurance for Clinical Radiotherapy Treatment Planning." *Medical Physics* 25.10 (1998): 1773-829.

4) Ezzell, Gary A., Jay W. Burmeister, Nesrin Dogan, Thomas J. LoSasso, James G. Mechalakos, Dimitris Mihailidis, Andrea Molineu, Jatinder R. Palta, Chester R. Ramsey, Bill J. Salter, Jie Shi, Ping Xia, Ning J. Yue, and Ying Xiao. "IMRT Commissioning: Multiple Institution Planning and Dosimetry Comparisons, a Report from AAPM Task Group 119." *Medical Physics* 36.11 (2009): 5359-373.

5) Oldham, Mark, Andrew Thomas, Jennifer O'Daniel, Titania Juang, Geoffrey Ibbott, John Adamovics, and John P. Kirkpatrick. "A Quality Assurance Method That Utilizes 3D Dosimetry and Facilitates Clinical Interpretation." *International Journal of Radiation Oncology*Biology*Physics* 84.2 (2012): 540-46.

6) Lee, Jeong-Woo, Semie Hong, Yon-Lae Kim, Kyoung-Sik Choi, Jin-Beom Chung, Doo-Hyun Lee, Bo-Young Choe, Hong-Seok Jang, and Tae-Suk Suh. "Effects of Static Dosimetric Leaf Gap on MLC-based Small Beam Dose Distribution for Intensity Modulated Radiosurgery." *Journal of Applied Clinical Medical Physics* 8.4 (2007): n. pag. Web.

7) Szpala, S., P. Atwal, F. Cao, and K. Kohl. "SU-E-T-455: Evaluation of the Influence of the Dosimetric Leaf Gap on RapidArc Plans Using Gafchromic

Film and Monte Carlo Simulations." *Medical Physics* 38.6 (2011): 3593. Web.

8) Rangel, A., N. Ploquin, I. Kay, and P. Dunscombe. "Towards an Objective Evaluation of Tolerances for Beam Modeling in a Treatment Planning System." *Physics in Medicine and Biology* 52.19 (2007): 6011-025. Web.

9) Moiseenko, Vitali, Vincent Lapointe, Kerry James, Lingshu Yin, Mitchell Liu, and Todd Pawlicki. "Biological Consequences of MLC Calibration Errors in IMRT Delivery and QA." *Medical Physics* 39.4 (2012): 1917. Web.

10) Rangel, Alejandra, and Peter Dunscombe. "Tolerances on MLC Leaf Position Accuracy for IMRT Delivery with a Dynamic MLC." *Medical Physics* 36.7 (2009): 3304. Web.

11) Rangel, Alejandra, Gesa Palte, and Peter Dunscombe. "The Sensitivity of Patient Specific IMRT QC to Systematic MLC Leaf Bank Offset Errors." *Medical Physics* 37.7 (2010): 3862. Web.

12) Tatsumi, D., M. N. Hosono, R. Nakada, K. Ishii, S. Tsutsumi, M. Inoue, T. Ichida, and Y. Miki. "Direct Impact Analysis of Multi-leaf Collimator Leaf Position Errors on Dose Distributions in Volumetric Modulated Arc Therapy: A Pass Rate Calculation between Measured Planar Doses with and without the Position Errors." *Physics in Medicine and Biology* 56.20 (2011): N237-246. Web.

13) Yan, Guanghua, Chihray Liu, Thomas Simon, Lee-Cheng Peng, Christopher Fox, and Jonathan Li. "On the Sensitivity of Patient-specific IMRT QA to MLC Positioning Errors." *Journal of Applied Clinical Medical Physics* 10.1 (2009): n. pag. Web.

14) Sakhalkar, H. S., J. Adamovics, G. Ibbott, and M. Oldham. "A Comprehensive Evaluation of the PRESAGE/optical-CT 3D Dosimetry System." *Medical Physics* 36.1 (2009): 71. Web.

15) Thomas, Andrew, Joseph Newton, John Adamovics, and Mark Oldham. "Commissioning and Benchmarking a 3D Dosimetry System for Clinical Use." *Medical Physics* 38.8 (2011): 4846. Web.

16) Clift, Corey, Andrew Thomas, John Adamovics, Zheng Chang, Indra Das, and Mark Oldham. "Toward Acquiring Comprehensive Radiosurgery Field Commissioning Data Using the PRESAGE®/ Optical-CT 3D Dosimetry System." *Physics in Medicine and Biology*55.5 (2010): 1279-293. Web.

17) Zhen, Heming, Benjamin E. Nelms, and Wolfgang A. Tome. “Moving from Gamma Passing Rates to Patient DVH-based QA Metrics in Pretreatment Dose QA.” *Medical Physics* 38.10 (2011): 5477. Web.

18) Nelms, Benjamin E., Heming Zhen, and Wolfgang A. Tome. “Per-beam, Planar IMRT QA Passing Rates Do Not Predict Clinically Relevant Patient Dose Errors.” *Medical Physics* 38.2 (2011): 1037. Web.

19) Arnfield, Mark R., Jeffery V. Siebers, Jong O. Kim, Qiuwen Wu, Paul J. Keall, and Radhe Mohan. “A Method for Determining Multileaf Collumator Transmission and Scatter for Dynamic Intensity Modulated RadioTherapy.” *Medical Physics* 27.10 (2000): 2231. Web.